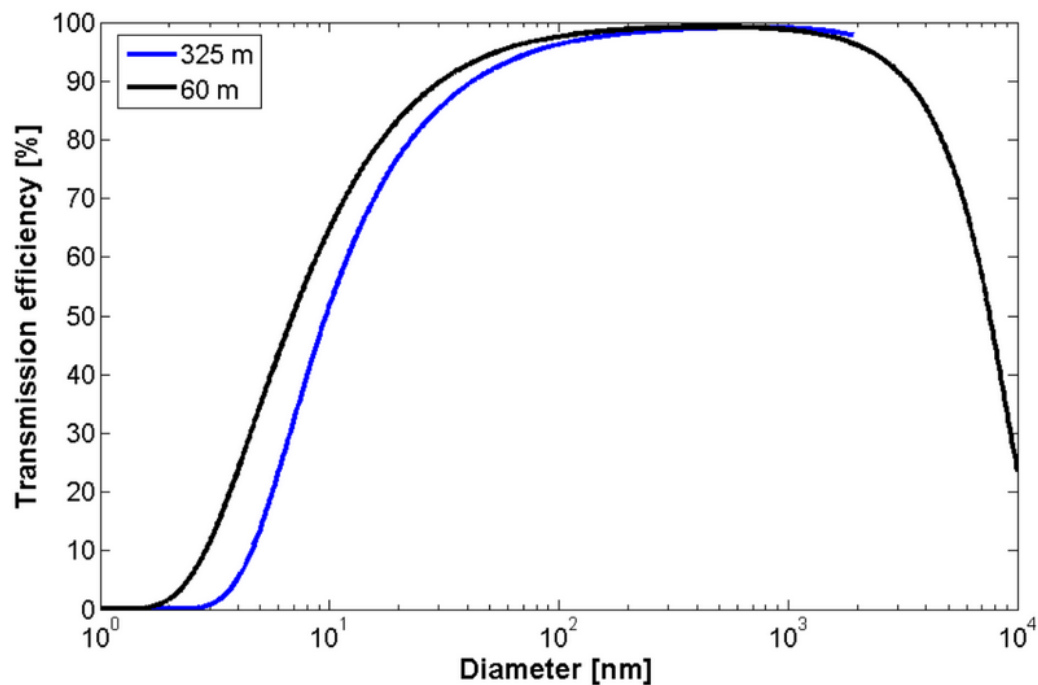


# *Vertically resolved aerosol variability at the Amazon Tall Tower Observatory under wet season conditions*

Franco et al.

Correspondence to: Marco Aurélio de Menezes Franco (marco.franco@usp.br), Christopher Pöhlker (c.pohlker@mpic.de)



**Figure S1.** Transmission efficiency curves obtained using the Particle Loss Calculator software, similarly to [Holanda et al. \(2023\)](#) for the 60 (black) and 325 m (blue) inlet lines.

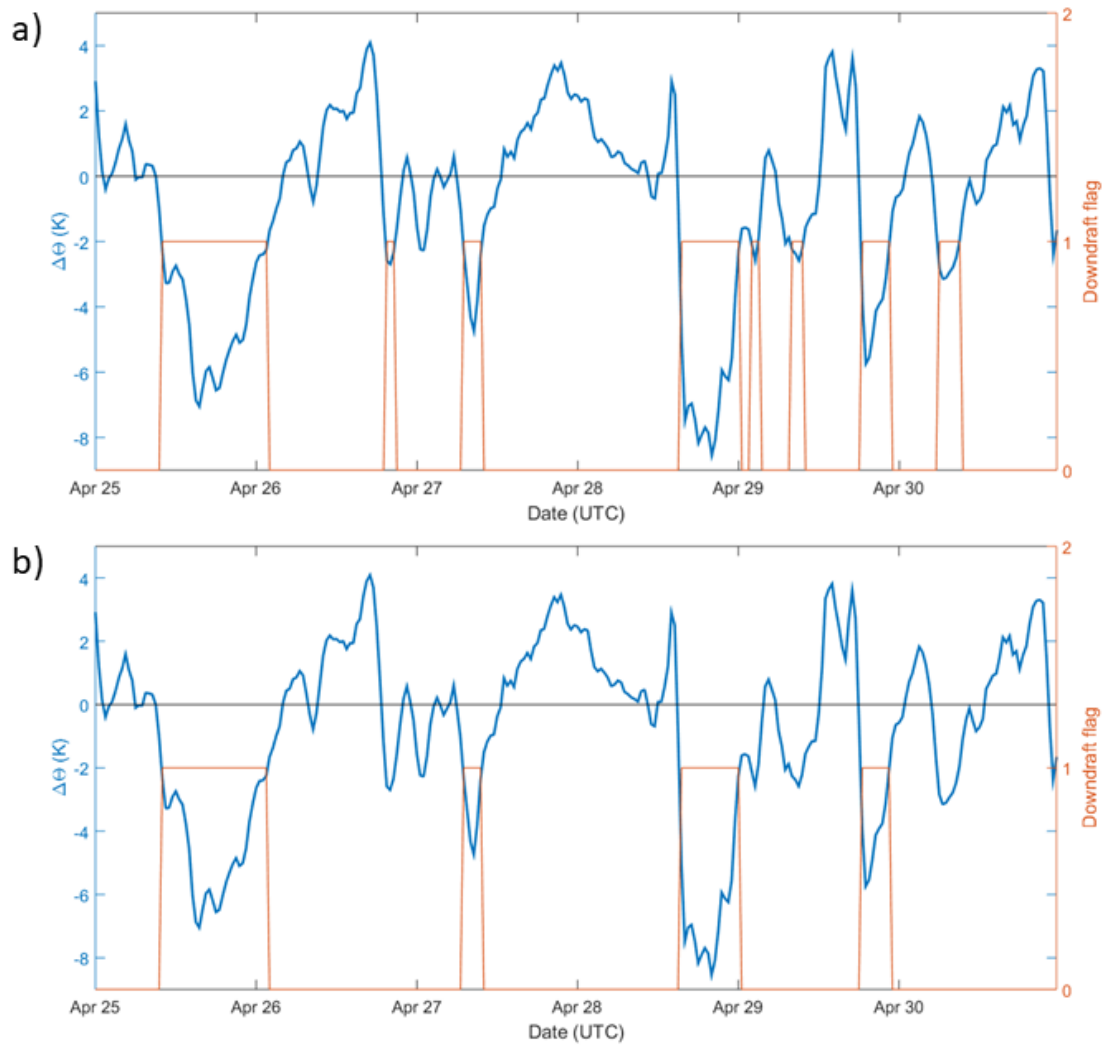


**Figure S2.** Examples of the use of the algorithm for downdraft detection, applied to 25-30 April 2020. In graph (a), all events are considered, and in graph (b), only the most intense events selected above the established threshold are detected. In both images, the blue curve represents the moving average of the potential temperature anomaly, and the orange peaks indicate the periods that the algorithm considered as belonging to a convective event. The horizontal black line indicates  $\Delta\theta = 0$ .

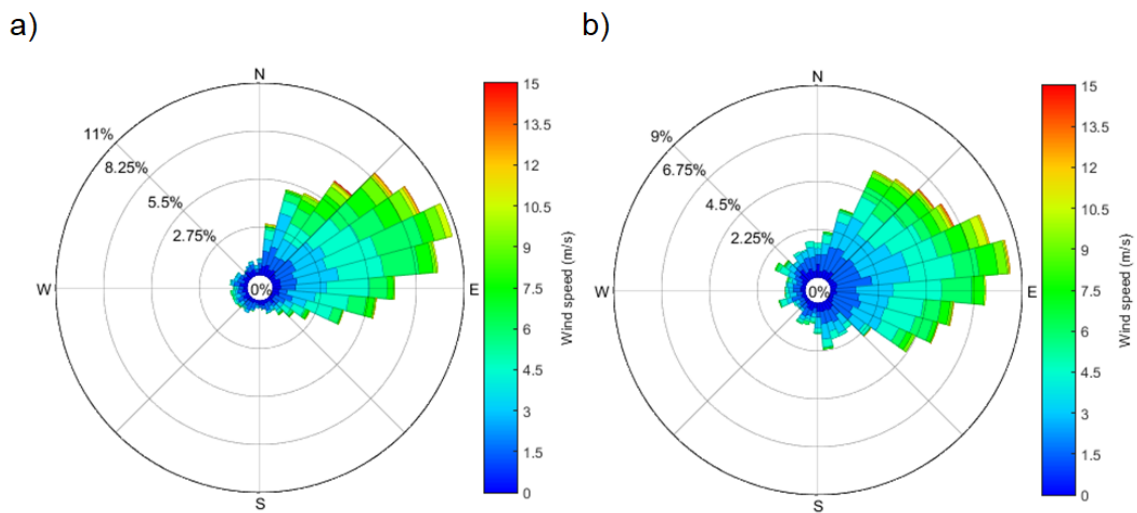


**Figure S3.** The wind rose for April and May a) 2019 and b) 2020. The colorbar expresses the wind speed (m/s), and the percentages in the figure represent the data coverage.

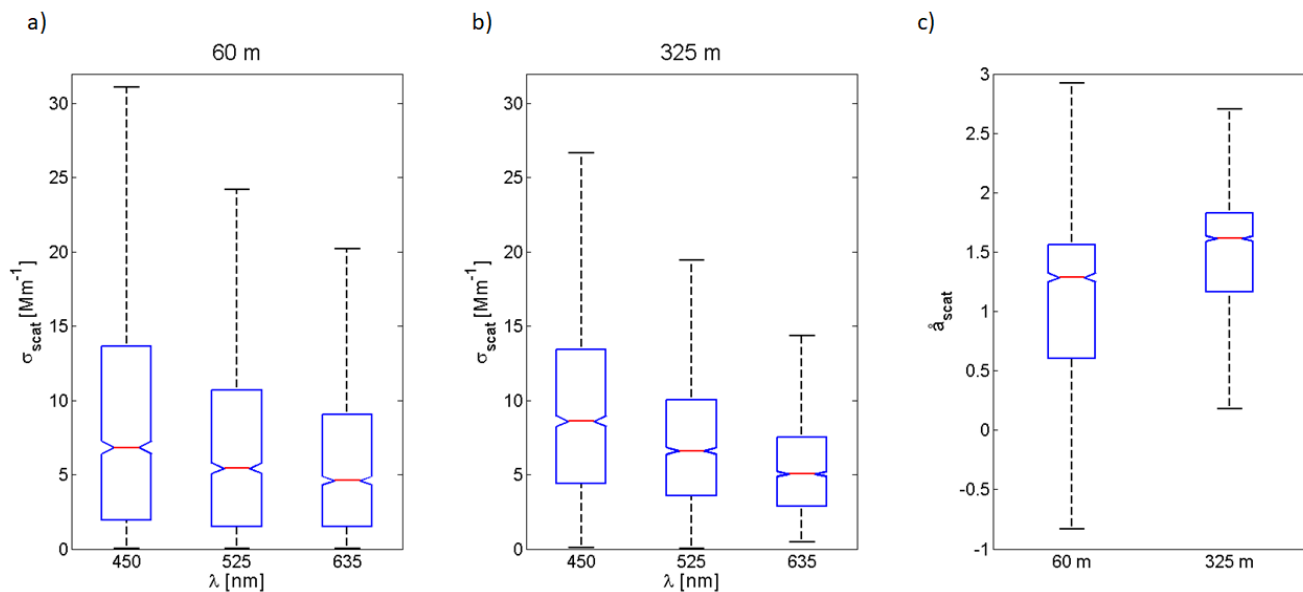


**Figure S4.** Comparative boxplots of aerosol scattering coefficients at wavelengths 450, 525, and 635 nm at a) 60 m and b) 325 m. In c), the comparative boxplot of the mean scattering Ångström exponent is presented. The box represents the quartiles, the whiskers represent the 90th and 10th percentiles, and the horizontal line represents the median.

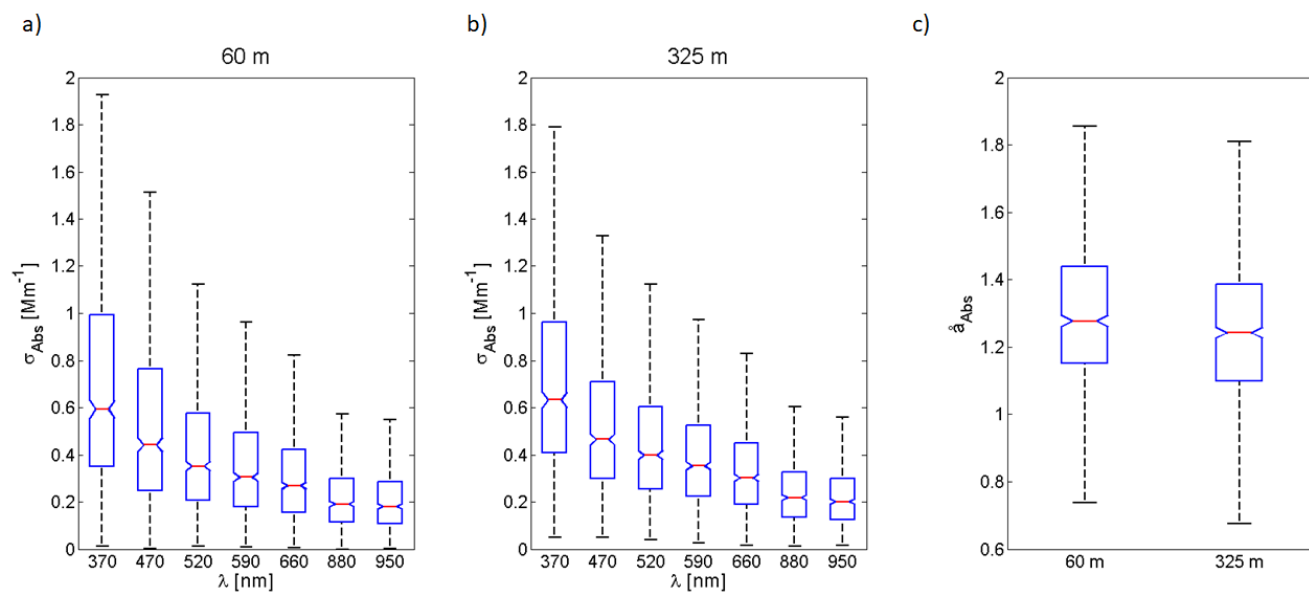


**Figure S5.** Comparative boxplots of aerosol absorption coefficients at  $\lambda = 370, 470, 520, 590, 660, 880$  and  $950$  nm at a) 60 and b) 325 m height. In c), the comparative boxplot of the mean absorption Ångström exponent is presented. The box represents the quartiles, the whiskers represent the 90th and 10th percentiles, and the horizontal line represents the median.

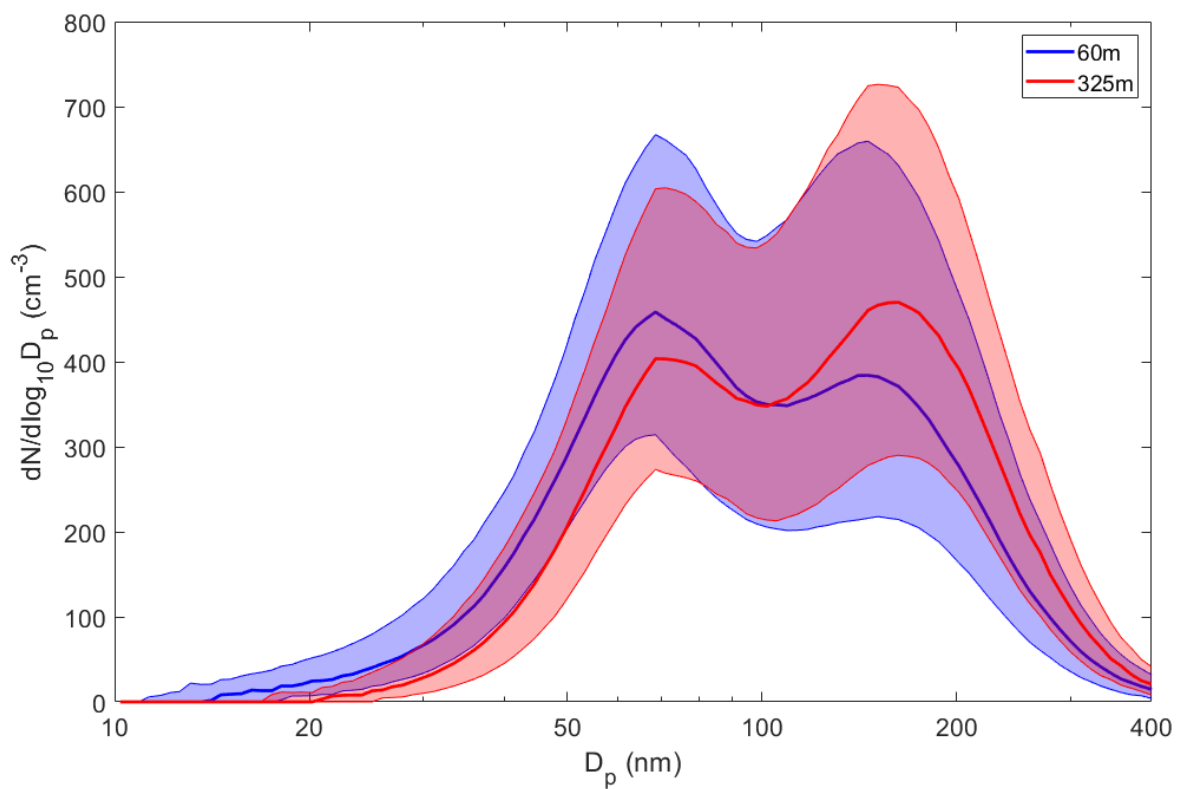


**Figure S6.** Median aerosol size distributions in the vertical profile. The blue line is the median aerosol size distribution at 60 m high, and the green line is the median aerosol size distribution at 325 m high. Colored shaded areas indicate the interquartile ranges.

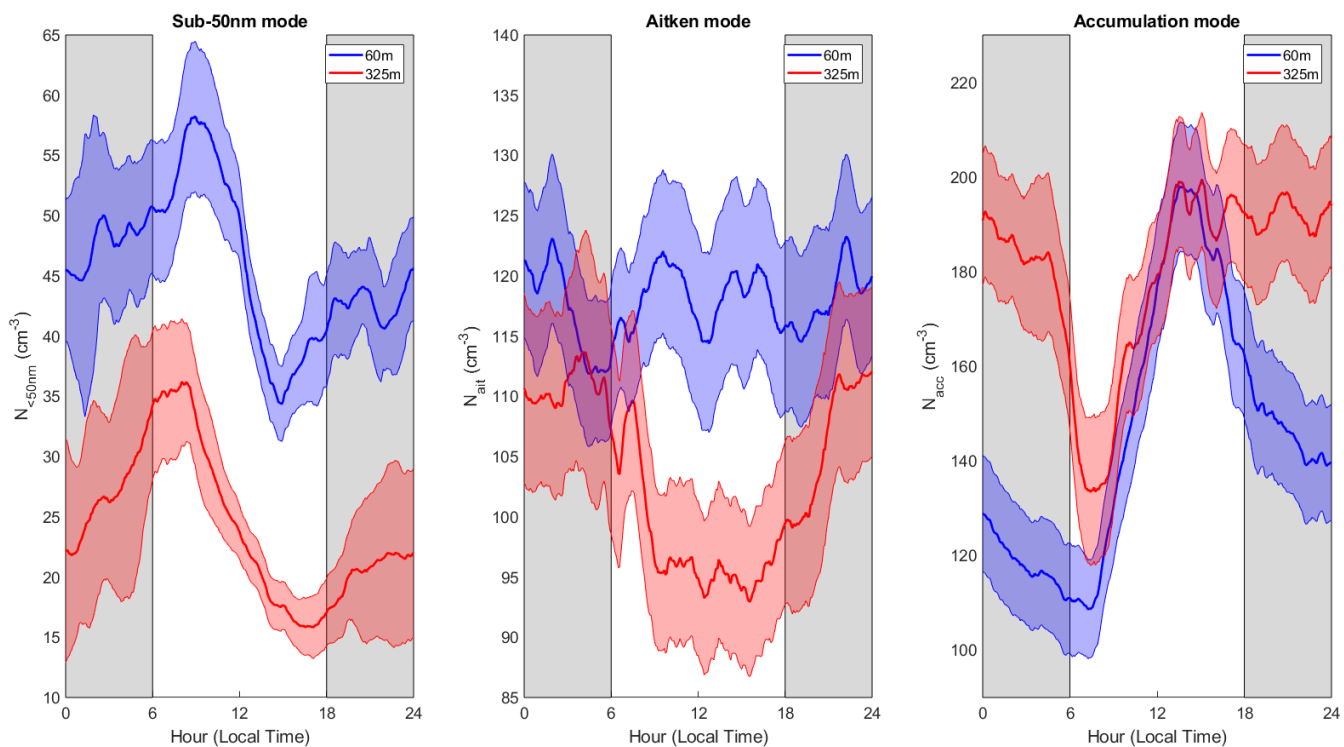


**Figure S7.** Median diurnal cycle of particle number concentrations in the a) sub-50 nm, b) Aitken, and c) accumulation modes. Bars are the standard error.

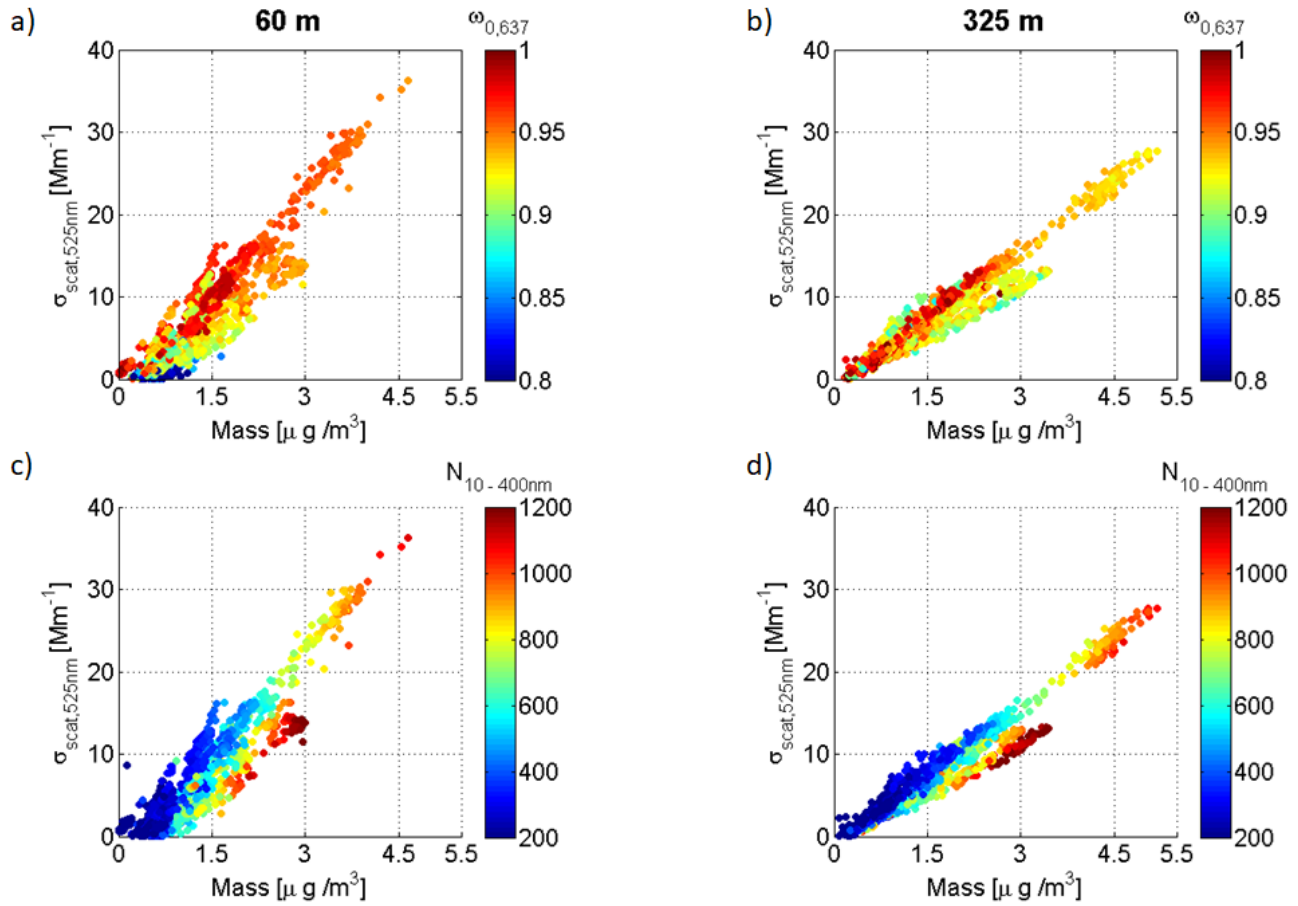


**Figure S8.** Scattering coefficient,  $\sigma_{\text{scat},525\text{nm}}$ , as a function of the mass concentration for measurements at 60 and 325 m height. The colors in panels a) and b) represent  $\omega_{0,637\text{nm}}$ , and the colors in c) and d) represent  $N_{10-400\text{nm}}$ . The mass concentration is obtained by multiplying the aerosol volume (in size range 10 to 400 nm) by the average mass loading of the wet season ( $1.4 \mu\text{g m}^{-3}$ ) (Artaxo et al., 2022)

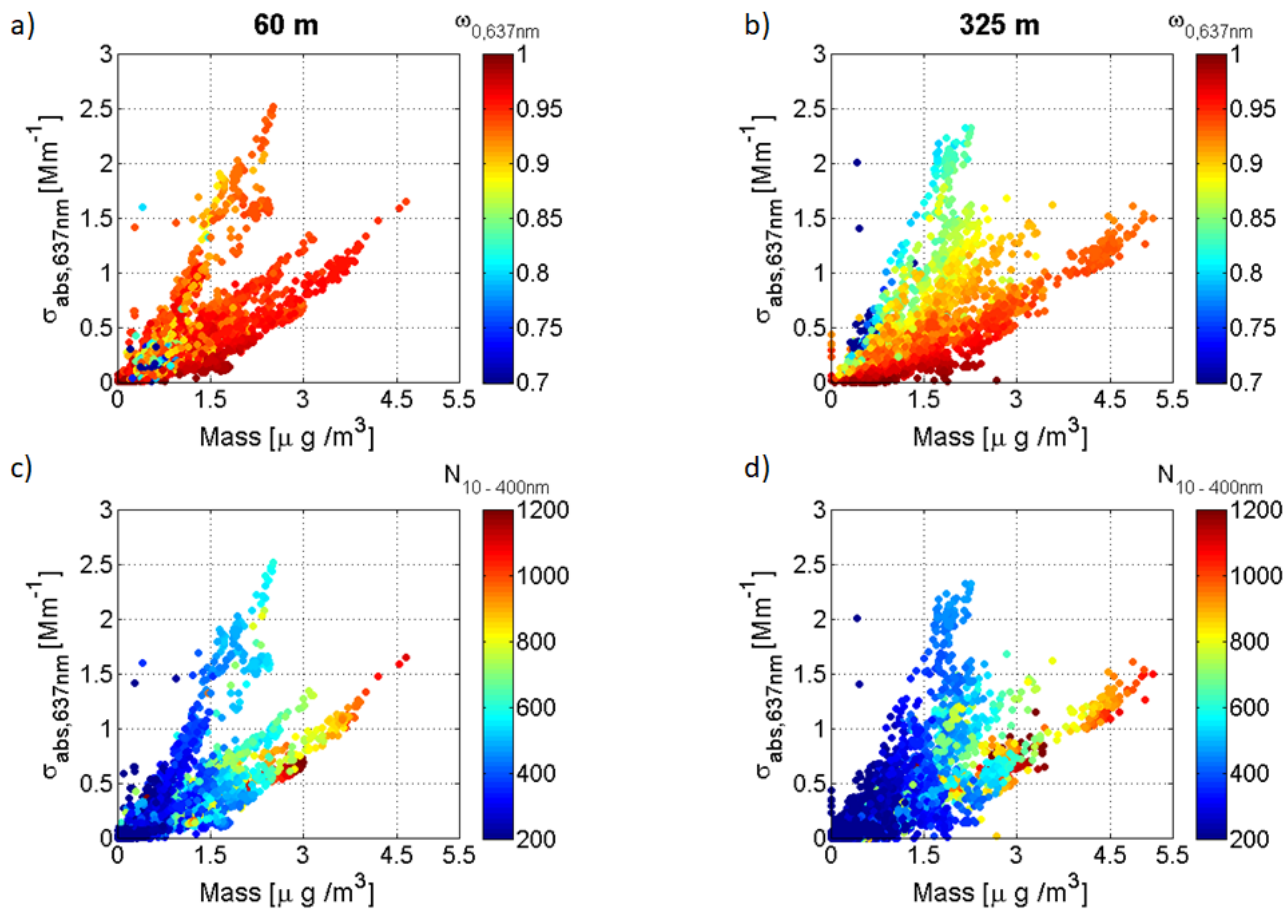


**Figure S9.** Absorption coefficient,  $\sigma_{abs,637nm}$ , as a function of mass concentration for measurements at 60 and 325 m height. The colors in panels a) and b) represent  $\omega_{0,637nm}$ , and the colors in c) and d) represent  $N_{10-400nm}$ . The mass concentration is calculated by multiplying the aerosol volume (within the size range of 10 to 400 nm) by the average mass loading of the wet season ( $1.4 \mu g m^{-3}$ ).



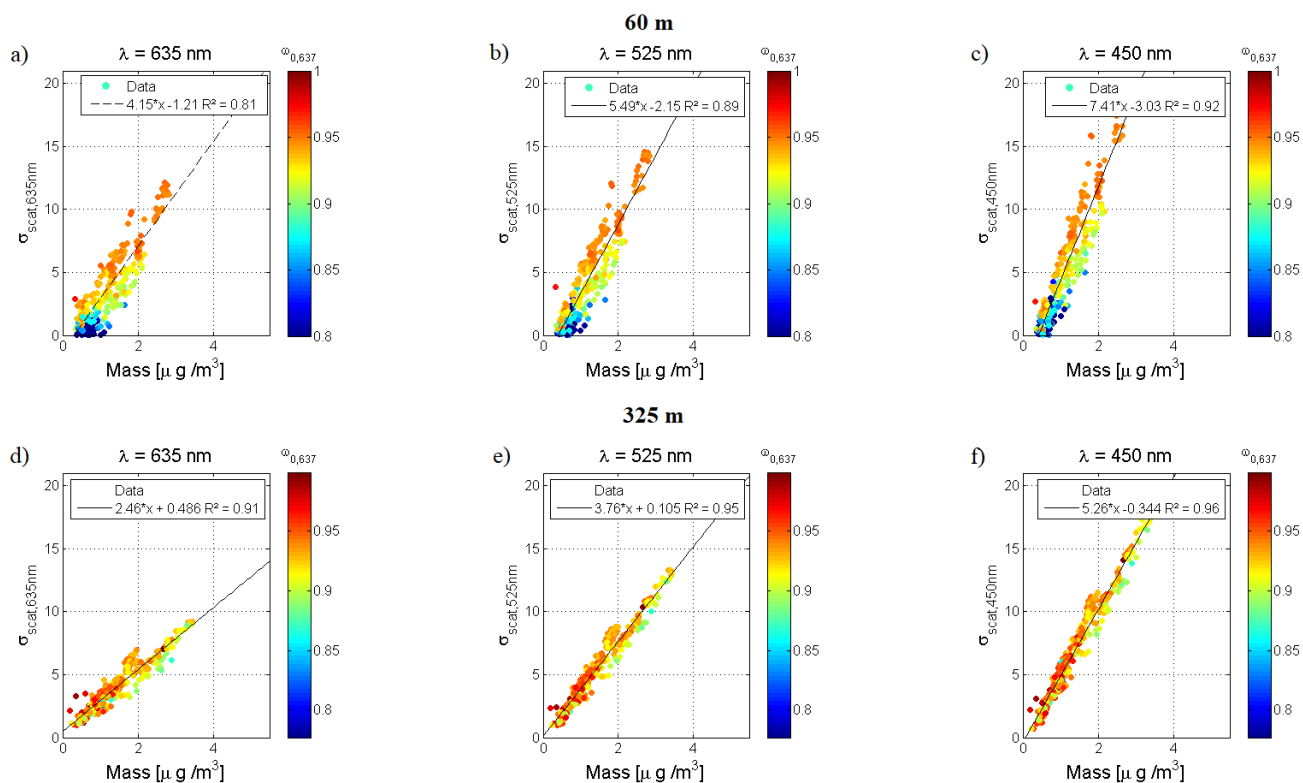


**Figure S10.** Spectral dependence of the scattering coefficient,  $\sigma_{scat}$ , as a function of mass concentration for measurements at 60 and 325 m height from 8 to 19 May 2019. Panels a), b) and c) represent the scattering coefficient measurements at 60 m height, and panels d), e) and f) represent measurements at 325 m height, at wavelengths of 635, 525, and 450 nm, respectively.

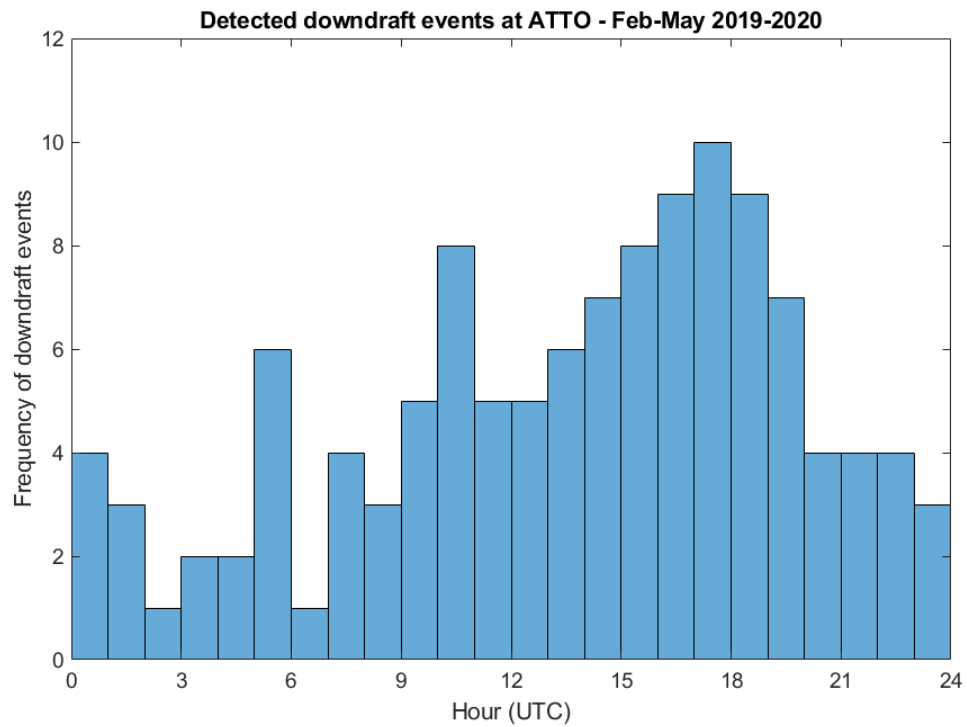


**Figure S11.** Histogram showing the starting hour of the detected intense downdraft events.

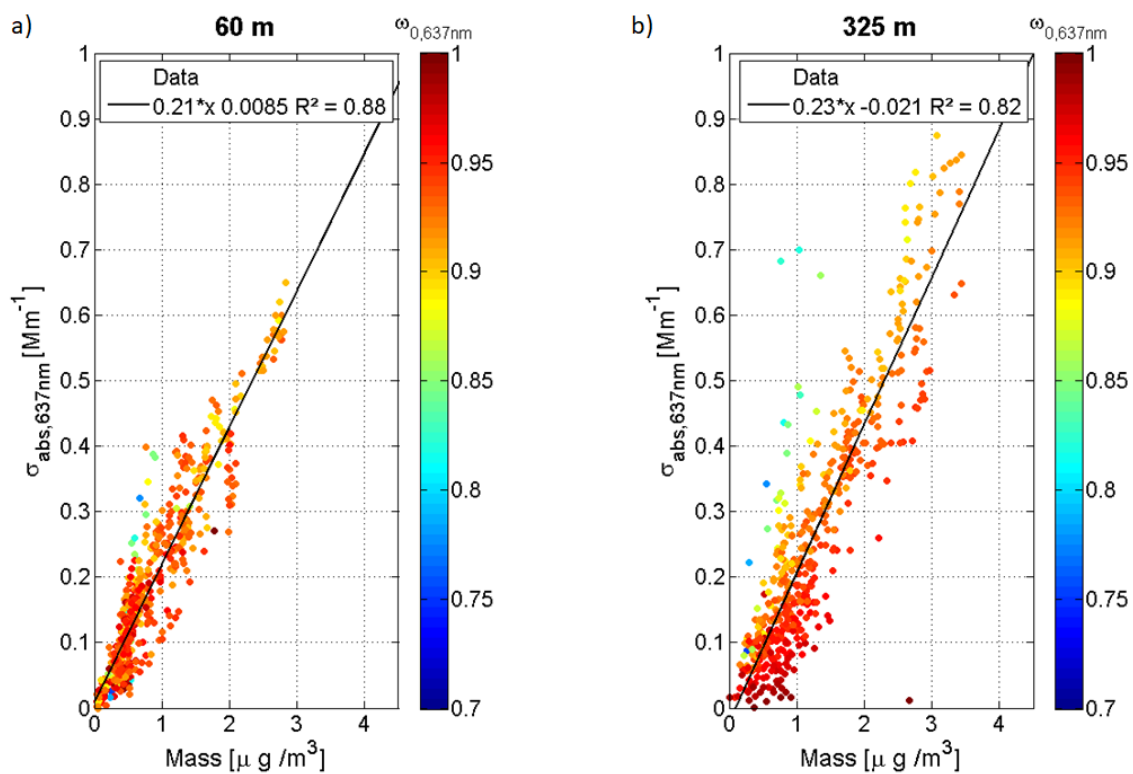


**Figure S12.** Total absorption coefficient,  $\sigma_{abs,637nm}$ , as a function of mass concentration for measurements at 60 and 325 m height. Panels a) and b) show the linear fits (black line) and the slopes ( $\alpha_{abs,637nm}$ ) for 60 and 325 m, respectively.

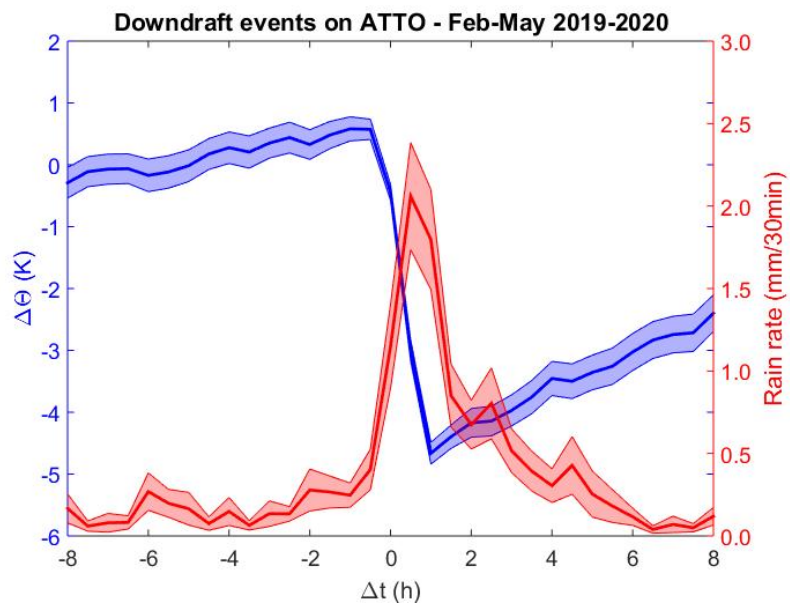


**Figure S13.** Composite analysis, considering the relative position of the data points to the onset of the closest detected downdraft event, for the potential temperature anomaly (blue) and precipitation rate (red) in a 16-hour window around the onset of downdraft events. The solid lines are the average values and the shaded areas represent the standard deviation of the mean.

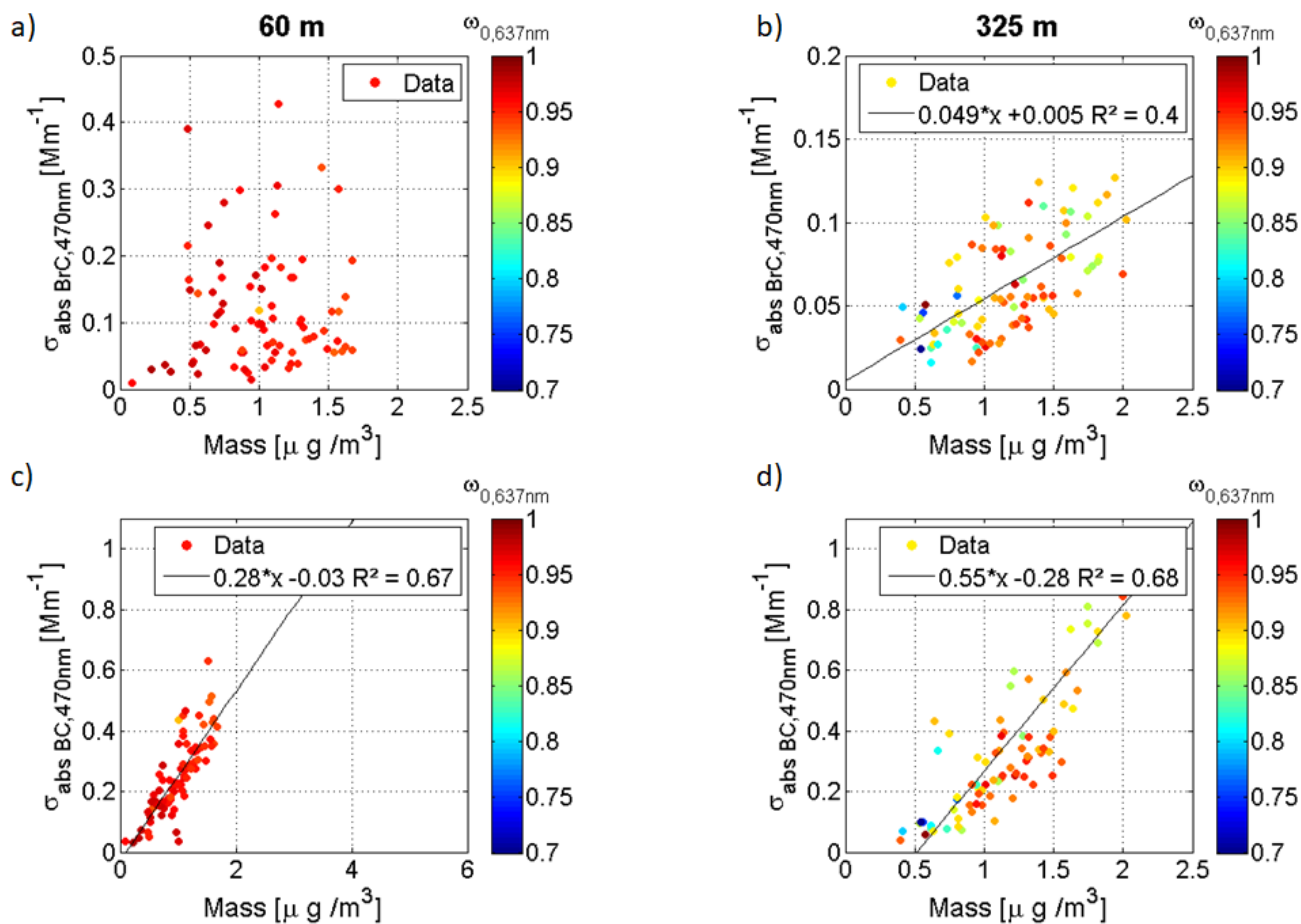


**Figure S14.** Absorption coefficient,  $\sigma_{abs,637nm}$ , as a function of mass concentration for measurements at 60 and 325 m height. Panels a) and c) show the linear fits (black line) and the slopes ( $\alpha_{abs,637nm}$ ) for BC and BrC absorption coefficients, respectively, at 60 m height, and panels b) and d) show the linear fits (black line) and the slopes ( $\alpha_{abs,637nm}$ ) for BC and BrC absorption coefficients, respectively, at 325 m height. Please note the different y-axes.